

Modelling the optical/UV emission of Swift J0243.6+6124 during its 2017–2018 giant outburst

J. Alfonso-Garzón,^{a,*} J. van den Eijnden,^b N. P. M. Kuin,^c F. Fürst,^d A. Rouco-Escorial,^e J. Fabregat,^f P. Reig,^{g,h} J. M. Mas-Hesse,^a P. A. Jenke,ⁱ C. Malacaria^j and C. Wilson-Hodge^k

^a*Centro de Astrobiología (CAB), INTA–CSIC,
ESAC, Camino Bajo del Castillo s/n, 28692 Villanueva de la Cañada, Spain*

^b*Department of Physics, University of Warwick,
Coventry CV4 7AL, UK*

^c*Department, University,
Holmbury St Mary, Dorking, Surrey RH5 6NT, UK*

^c*Mullard Space Science Laboratory,
Street number, City, Country*

^d*Quasar Science Resources SL for ESA,
European Space Astronomy Centre (ESAC), 28692 Villanueva de la Cañada, Madrid, Spain*

^e*European Space Agency (ESA),
European Space Astronomy Centre (ESAC), Camino Bajo del Castillo s/n, 28692 Villanueva de la Cañada, Spain*

^f*Observatorio Astronómico, Universidad de Valencia,
Catedrático José Beltrán 2, 46980 Paterna, Spain*

^g*Institute of Astrophysics, Foundation for Research and Technology-Hellas,
71110 Heraklion, Greece*

^h*Physics Department, University of Crete,
71003 Heraklion, Greece*

ⁱ*University of Alabama in Huntsville,
Huntsville, AL 35805, USA*

^j*International Space Science Institute,
Hallerstrasse 6, 3012 Bern, Switzerland*

^k*ST12 Astrophysics Branch, NASA Marshall Space Flight Center,
Huntsville, AL 35812, USA*

E-mail: julia@cab.inta-csic.es

*Speaker

The Be X-ray binary Swift J0243.6+6124 underwent a super-Eddington giant outburst that lasted from September 2017 to February 2018. The reached luminosity was so high, that it became the first Ultraluminous X-ray pulsar (ULXP) in the Galaxy. Simultaneously to this X-ray outburst, optical and UV outbursts were observed. In this work, we try to explain the origin of this emission. We built a physical model considering the heating of the surface of the Be star, the emission from the viscously heated accretion disk, and the irradiation of this accretion disk by the central X-ray source. Using this model, we fit the Spectral Energy Distributions built with the available photometric measurements obtained each day along the outburst.

1. Introduction

Be/X-ray binaries (BeXRBs) are systems in which a neutron star (NS) orbits around a Be star [28]. BeXBs can exhibit two types of outbursts: type I or normal outbursts, with moderate intensity outbursts ($L_X \approx 10^{36} - 10^{37} \text{ erg s}^{-1}$), and type II or giant outbursts, with ($L_X > 10^{37} \text{ erg s}^{-1}$). Type I or normal outbursts always occur close to the periastron passage of the NS, when the NS approaches the periastron of the system and interacts with the Be circumstellar disc. Type II outbursts can occur at any orbital phase and their origin remains unclear.

Swift J0243.6+6124 is a unique system. It was first detected by the Burst Alert Telescope (BAT) on board the Neil Gehrels *Swift* observatory on 3rd October 2017 during a giant X-ray outburst [20]. Timing analysis revealed a periodicity at 9.86s, suggesting that the new transient is an X-ray pulsar. Pulsations were subsequently confirmed by Fermi [19] and NuSTAR [3]. The Fermi/GBM accreting pulsar observations allowed accurate determination of the orbital period $P_{orb}=27.587 \text{ d}$ and eccentricity $e=0.098$ [40, 42]. A detailed analysis of the spectral and photometric characteristics of the optical counterpart of Swift J0243.6+6124, which was classified as a O9.5Ve star, was performed by Reig et al. [29]. It is the first and only ultra-luminous X-ray pulsar in our Galaxy and it was the first high-mass Be X-ray pulsar showing radio jet emission [34].

During its only super-Eddington giant X-ray outburst in 2017–2018, the source displayed unprecedented bright emission in the UV and optical wavelengths tightly correlated with the X-ray behaviour [29]. In this work, the analysis of the optical/UV emission is presented.

2. Observations

We have combined optical photometry in the *V*-Johnson band from several observatories (see Reig et al. [29] for details on the dataset and Fig. 1). Apart from these observations, we have also used multi-colour photometry from the Ultra-Violet/Optical Telescope (UVOT, Roming et al. 31) on board the *Neil Gehrels Swift Observatory* [hereafter *Swift*; 14] instrument. The optical/UV light curves of Swift J0243.6+6124 are shown in Fig. 2.

In order to characterise the X-ray evolution throughout the outburst, we used the data from both the X-ray Telescope [XRT; 5] and the Burst Alert Telescope [BAT; 4]. We extracted and analysed all the XRT available spectra using the *Swift* online data reduction pipeline [11, www.swift.ac.uk/user_objects/] for all observations of the 2017/2018 outburst. For *Swift*/BAT, we downloaded the daily source count rates from the Hard X-ray Transient Monitor webpage [22, <https://swift.gsfc.nasa.gov/results/transients/>]. The BAT light curve is shown in navy blue in Fig 1.

3. Data analysis

3.1 Isolation of the extra optical/UV emission due to the outburst

Clear long-term variability can be observed in the *V*-Johnson band light curve shown in Fig. 1. This oscillation has a quasi-period of ~ 1200 days. Same type of variability was observed in the WISE light curves in Reig et al. [29], the amplitude of the variability being larger for longer wavelengths. These modulations can be explained by the replenishment and dissipation of the

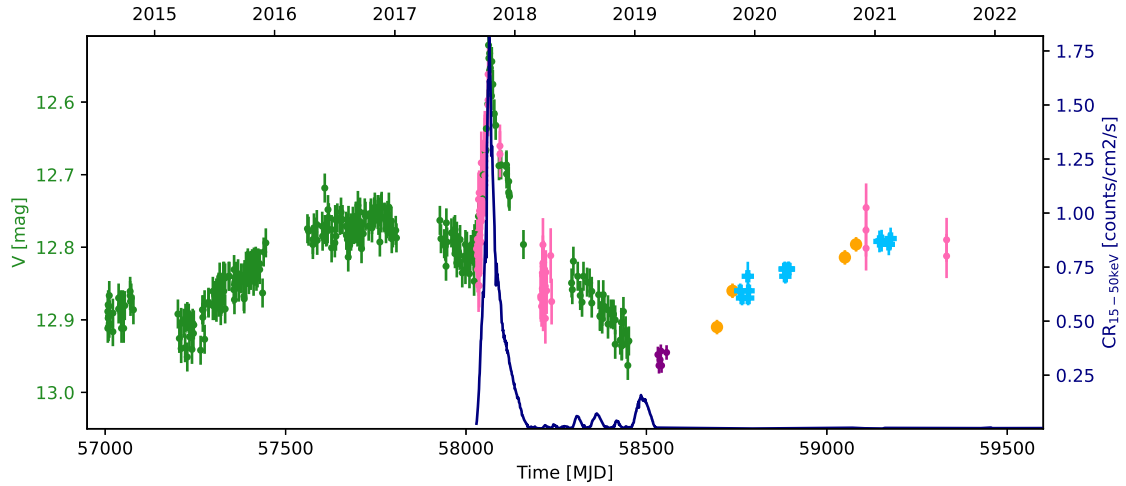


Figure 1: Optical vs X-ray long-term light curves of Swift J0243.6+6124. the light curve contains observations from different sites: green points come from ASAS–SN Variable Stars Database, pink points correspond to converted *Swift*/UVOT–*v* observations, purple points are from AAVSO, orange points are from Skinakas observatory, and light blue points are from Aras de los Olmos Observatory (see Reig et al. [29] for details). The navy blue line represents the X-ray count rate light curve measured with *Swift*/BAT in the 15–50 keV band.

circumstellar disk, and this explanation is in agreement with the evolution of the $\text{EW}(\text{H}\alpha)$ line [24, 29]. In order to have an estimation of the emission from the Be star and the circumstellar disk in the *V*–Johnson band, we performed a cubic spline fit to the points outside the outburst (we did not consider the points between MJD 57850 and 58300 MJD) on the long-term *V*–Johnson light curve. For the other optical and UV bands for which the temporal coverage was poorer, we just performed a linear fit to those points out of the outburst between MJD 58200–58300 (epoch when it is considered that the giant outburst ended) and MJD 58500–58600 (epoch when the minimum fluxes were measured at all the wavelengths). Then we subtracted this linear fit from the observed fluxes along the outburst.

The long-term light curves of the fluxes (de-reddened for an $E(B-V)=1.2$ mag, assuming the extinction law from Fitzpatrick [12]), in the six UV/optical filters are shown in Fig. 2. The estimation of the Be+disk emission at each wavelength is plotted with a gray dashed line. The variations due to changes in the circumstellar disk are larger for redder wavelengths (as can be seen from the slopes of the fits in Fig. 2).

We used these residuals (after subtracting the Be+disk component) to build the daily optical/UV SEDs that trace the emission exclusively due to the outburst. These SEDs will be shown and studied in Sect. 4.2.2.

3.2 Estimation of the X-ray fluxes

We fitted each XRT spectrum with a combined absorbed power law plus black body model, scripting the automatic fit for each spectrum in *xspec* [2]. We assumed interstellar abundances from Wilms et al. [39] and cross-sections from Verner et al. [37]. We used the *tbnew*, *pegpwr1w*, and

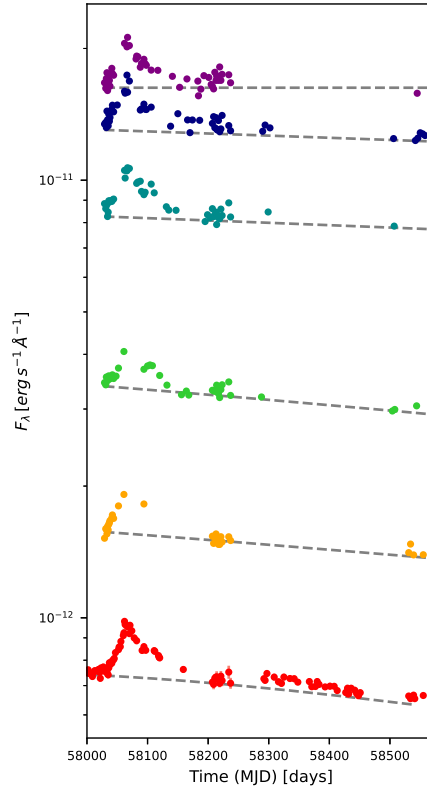


Figure 2: Light curves of the de-reddened monochromatic fluxes in the optical and UV light curves of Swift J0243.6+6124. From top to bottom: UVOT-*uw2*, UVOT-*um2*, UVOT-*uw1*, UVOT-*u*, UVOT-*b*, and Johnson *V*. Monochromatic fluxes have been dereddened with $E(B-V)=1.2$ mag. The dashed gray lines represent the fits used to model the Be+circumstellar disk contribution.

bbodyrad models of *xSPEC*. In all fits, the neutral hydrogen absorption column density was fixed to $N_H = 0.825 \times 10^{22} \text{ cm}^{-2}$. We have calculated this quantity considering the relation between N_H and A_V given by Güver & Özel [16], for a value of the optical extinction $A_V = R_V * E(B-V) = 3.7$ mag (see Alfonso-Garzón et al. [1] for details). From the *Swift*/XRT spectral fit, we obtained the fluxes in 0.5–2 keV and 2–10 keV bands that will be used to calculate the correlation indexes in Sect. 3.4.

To obtain bolometric fluxes from the *Swift* monitoring, however, the spectral cutoff at higher energies needs to be corrected. Therefore, we combined the above *Swift*/XRT fits with the measured 15–50 keV count rates from the *Swift*/BAT hard X-ray transient monitor. As the spectral shape changes during the outburst, we cannot simply apply a single, constant conversion factor between the BAT count rate and flux. Instead, we took the best-fit XRT spectral model for each observing date and then added a high-energy exponential cutoff (*highcut* model in *xSPEC*).

The light curves of the residual optical emission in the *V*–Johnson band obtained from the calculations described in Sect. 3.1, along with the X-ray light curve of the Swift J0243.6+6124 outburst, converted to luminosities considering a distance of $d=5.2$ kpc, are shown in Fig. 3. A clear correlation between the optical and X-ray fluxes is observed, although this correlation differs between the rise and the decay of the outburst.

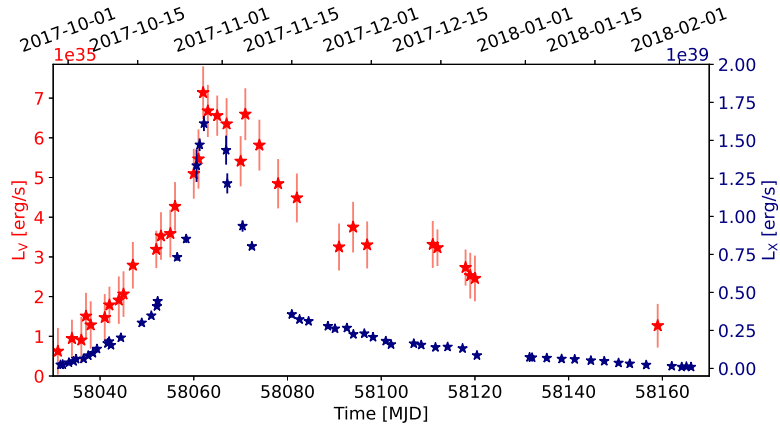


Figure 3: Optical (red) vs X-ray bolometric (navy blue) emitted luminosities during the bright outburst of Swift J0243.6+6124. The optical V -band integrated fluxes have been obtained multiplying the monochromatic fluxes (converting magnitudes to fluxes with a zeropoint $ZP=3.631 \times 10^{-9} \text{ erg s}^{-1} \text{ cm}^{-2} \text{ mag}^{-1}$) by the effective width of the filter (890 \AA) and dereddened considering $E(B-V)=1.20 \text{ mag}$. A distance $d=5.2 \text{ kpc}$ has been assumed in the luminosity calculations ($L = 4\pi d^2 \times F$).

3.3 Timescales of the light curves decays

When reprocessing dominates the optical emission during X-ray outbursts of X-ray binaries, the exponential decay timescales of the optical and IR light curves should be 2–4 times longer than the X-ray value [21, 32]. An exponential decay can be observed for Swift J0243.6+6124 in Fig. 3.

We have calculated the decay of the outburst in our X-ray, UVOT- $uw2$, UVOT- $um2$, UVOT- $uw1$, and V -Johnson light curves, by fitting the formula $F = F_0 e^{-t/\tau}$ to our observations, and the results of these fits are shown in Table 1. We could not fit the UVOT- u and UVOT- b light curves due to the poor temporal coverage of the outburst decay that did not allow to correctly perform the fit.

Table 1: Timescales of the decay of the giant outburst for the X-ray, UVOT- $uw2$, UVOT- $um2$, UVOT- $uw1$, and V -Johnson light curves, as a result of fitting the formula $F = F_0 e^{-t/\tau}$ to the observed light curves.

$\tau_{0.1-500 \text{ keV}}$	τ_{UW2}	τ_{UM2}	τ_{UW1}	τ_V
$13 \pm 1 \text{ d}$	$22 \pm 3 \text{ d}$	$21 \pm 3 \text{ d}$	$40 \pm 3 \text{ d}$	$42 \pm 3 \text{ d}$

The decay timescales of the optical (V -Johnson band) and UVOT- $uw1$ light curves are ~ 4 times the decay timescale of the X-ray light curve. However, the decay timescales of the UVOT- v and UVOT- $uw1$ light curves are ~ 2 times the decay timescale of the X-ray light curve.

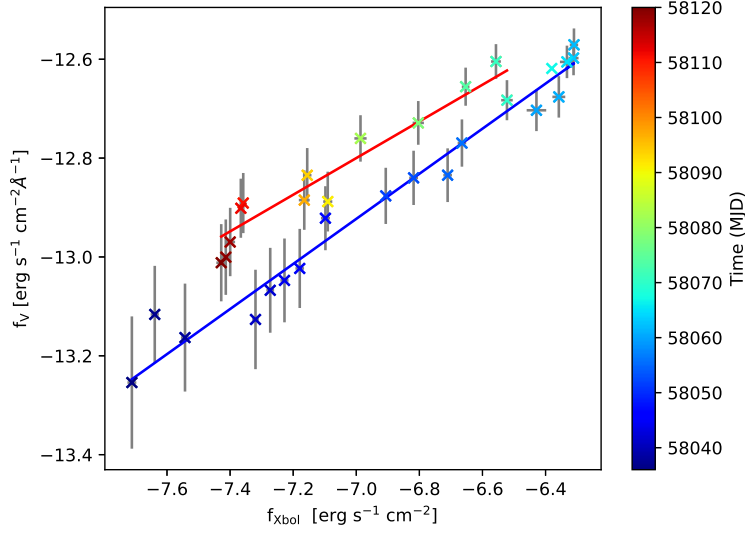
3.4 Flux-flux correlations

The relationship between the optical (V -Johnson filter) and the bolometric X-ray fluxes (0.1–500 keV) in Swift J0243.6+6124 during the rise and decay of the outburst is represented in Fig. 4.

Table 2: Slopes of the correlations between the optical fluxes in the V–Johnson band and the X-ray fluxes in different bands, $F_V \propto F_X^\beta$, during the rise and decay of the outburst.

	$\beta_{0.1-500\text{ keV}}$	$\beta_{0.5-2\text{ keV}}$	$\beta_{2-10\text{ keV}}$	$\beta_{15-50\text{ keV}}$
Rise	0.56 ± 0.03	0.40 ± 0.02	0.47 ± 0.02	0.90 ± 0.02
Decay	0.37 ± 0.03	0.26 ± 0.02	0.31 ± 0.02	0.59 ± 0.04

A linear correlation is clearly observed, although the slope is steeper during the rise than during the decay. The correlation indexes between the optical and X-ray fluxes, varying the X-ray energy band are listed in Table 2. We have also observed that this slope depends on the energy band used to estimate the X-ray flux, increasing when harder X-rays are used. Despite this effect, in all cases a steeper slope is observed during the rise than during the decay. This is in agreement with the fact that the time scales of the decay are longer in the optical than in X-rays.

**Figure 4:** Optical/X-ray (0.1–500 keV) flux-flux correlations during the giant outburst of Swift J0243.6+6124. The linear fits to the data show different slopes during the outburst rise (blue line) and decay (red line) phases.

4. Results and discussion

In this section, we will discuss first the possible mechanisms that can explain the observed UV/optical fluxes, considering the results obtained in Sect. 3. Then we will model the most relevant effects in order to reproduce the evolution of the SED along the outburst in correlation with the X-ray emission. We will discuss the possible interpretations of the results of the SED fits. Finally, we will provide some possible explanations to the optical/UV humps observed during the decay of the outburst.

4.1 Origin of the optical/UV emission

There are several mechanisms that can contribute to the optical/UV emission and display similar amplitude variability in X-ray binaries, including the formation and dissipation of the Be circumstellar disk and/or the changes in the inclination, warping and/or precession of this circumstellar disk [26, 41], mass ejections from the Be star [30], or directly the jet, given the fact that this was the first Be X-ray binary for which signatures from a jet has been found [34]. We have analysed these mechanisms, concluding that their predictions do not fit the observational properties of the Swift J0243.6+6124 outburst (see Alfonso-Garzón et al. [1] for details).

On the other hand, there are other mechanisms that could lead to optical/UV emission directly related with the X-ray emission we have considered in order to explain the optical and UV fluxes observed during this outburst. These mechanisms are: *a*) thermal emission from the viscously heated accretion disk around the NS, *b*) reprocessing of the hard X-rays in the accretion disk, *c*) X-ray heating of the surface of the Be star. Given the tight correlation observed between the X-ray and optical/UV fluxes, some of these X-ray related mechanisms could be significantly contributing to the optical and UV emission observed during the giant X-ray outburst of Swift J0243.6+6124. The UV and optical timescales calculated in Sect. 3.3 are in the range 2–4 times the X-ray decay timescale (see Table 1), so according to King & Ritter [21], these results favour the X-ray reprocessing as the main mechanism contributing to the UV and optical variability observed during the outburst.

The correlation indexes obtained from the flux-flux correlation analysis ($F_V \propto F_X^\beta$) are shown in Table 2. Some of the obtained indexes, would be in agreement with the correlation index typical of X-ray reprocessing proposed by van Paradijs & McClintock [35], $\beta=0.5$. However, these indexes are larger for the rise than for the decay of the outburst and vary with the considered X-ray energy band. The dependence on the energy band could be related to the changes in the X-ray spectra, and the variable contribution from the reflected emission during the Super-Eddington state [6]. Also the fact that the albedo is expected to vary with energy of the X-ray impinging radiation could affect the correlations (harder X-rays penetrate more in the disk). The differences between the rise and decay could be related to the presence of a more extended accretion disk during the decay than during the rise, or if the disk gets flared along the outburst. Moreover, the source underwent different accretion regimes, from sub- to super-critical accretion, and to a third regime with a radiation-pressure dominated accretion disk [8], and this could also affect the correlations. As mentioned by Gierliński et al. [15], these simple flux-flux correlations alone can be inaccurate to explain in detail the origin of the optical/UV emission for individual LMXBs. For HMXBs, the analysis can be even more complicated. For this reason, we tried a different approach involving a more complex modelling of the emission mechanisms that will be presented in Sect. 4.2.

4.2 SED modelling through the outburst

Since the effects directly related to the X-ray emission seem to be the most plausible mechanisms driving the optical/UV emission observed during the giant outburst of Swift J0243.6+6124, we have created a physical model considering the following mechanisms: emission from the viscously heated accretion disk, emission coming from the X-ray irradiation of the accretion disk, and emission due to the heating of the surface of the companion star. We have modelled these effects and used

the calculated fluxes in each optical/UV filter to build a theoretical SED to be compared with the observed optical/UV SEDs.

4.2.1 Description of the model

In all the calculations, we have used a distance of $d = 5.2$ kpc to estimate the X-ray incident luminosities (which is an input for the three models), and to convert the calculated optical/UV luminosities to fluxes so that they can be compared with the observed SEDs.

We have used the most recent orbital parameters provided in the GBM Accreting Pulsar Histories web accesible at <https://gammarray.nsstc.nasa.gov/gbm/science/pulsars/lightcurves/swiftj0243.html> of the GBM Accreting Pulsars Program (GAPP, Malacaria et al. 25). We then used an orbital period $P_{orb} = 27.698899$ days, a projected semi-major axis $a \sin i = 115.531$ light-sec, an eccentricity $e = 0.1029$, and a binary epoch $T_{\pi/2} = 2458116.09700$ JED. On the other hand, we considered an inclination of the orbit of $i = 30^\circ$ [29].

For each day of the outburst (whenever we had some optical/UV observation), we used the X-ray luminosity extracted from linear interpolation of the X-ray bolometric fluxes in the light curve generated from the method described in Sect. 3.2, to be used as an input of the different parts of the model. The XRT spectra (purple line) and the models used to fit them for on day of the outburst (58094 MJD), are plotted in Fig. 5. The blackbody components are plotted with light blue dotted lines and the power laws are plotted with navy blue dashed lines.

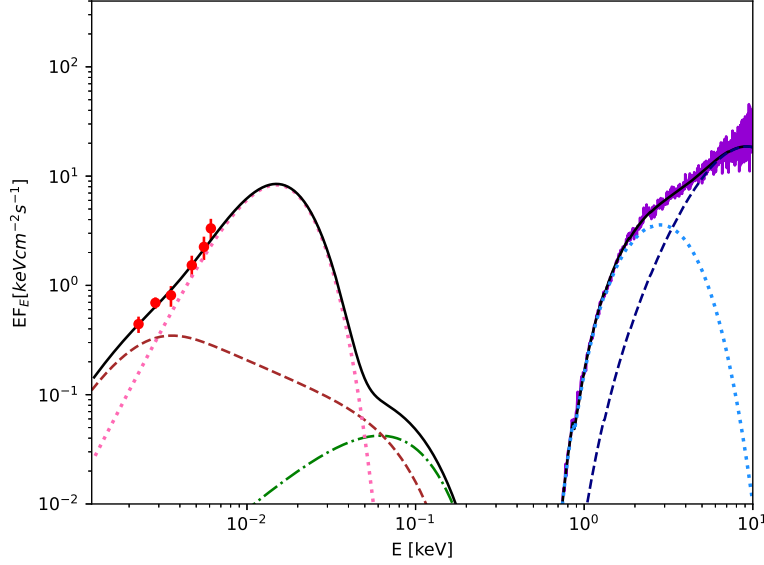


Figure 5: Models considered in this work to fit the optical/UV observations (red points) and XRT spectra (purple line) for 58094 MJD. The contribution of X-ray heating of the companion star is represented with a pink dotted line, the irradiated disk is plotted as a brown dashed line, the viscously heated disk is plotted with a green dash-dotted line. The xspec models `bbbodyrad` and `pegpowerlaw` used to fit the XRT spectra are plotted with light blue dotted and navy blue dashed lines respectively.

For the two mechanisms involving the accretion disk, we performed two different fits. In the first one, we left the outer radius R_{out} as a free parameter, using a grid with step $0.01a$, and taking

values from $R_{out}=0.01a$ to $R_{out}=0.20a$ (typical predicted sizes of an accretion disk according to theoretical models are $R_{out} = 0.04 - 0.10a$, see for example Hayasaki & Okazaki [17, 18]), being a the semi-major axis of the orbit. We have set an upper limit of R_{out} based on the size of the Roche lobe. For a mass of the donor star of $M_*=18 M_\odot$ and considering the mass of the NS $M_{NS}=1.4 M_\odot$, and using the approximation by Eggleton [10], we got a value of the Roche lobe of $R_L=0.20a$. For the second fit, we fixed $R_{out} = 0.20a$ and fit a factor dependent on other effects that will be explained later. For each accretion rate, we approximated the inner radius of the accretion disk as the magnetospheric radius, calculated considering a magnetic field of $B\sim 6.6*10^{12}G$ (value obtained from the estimation by Wilson-Hodge et al. [40], $B\sim 1 \times 10^{13}$ (d/7kpc) G). To estimate r_m we used the following equation [13]:

$$r_m = \dot{M}^{-2/7} \mu^{4/7} (GM)^{-1/7} 2^{-3/7} \quad (1)$$

The accretion rate (\dot{M}) has been obtained from the X-ray bolometric luminosity using the formula:

$$L_X = \frac{GM\dot{M}}{R} \quad (2)$$

and considering typical values of a NS of $M = 1.4 M_\odot$ and $R = 10^6$ cm.

The specific models we considered for each of these three mechanisms are described below. These components of the model used to fit the optical/UV observations (red points), are plotted in Fig. 5.

- Emission from the viscously heated accretion disk:

We modelled the contribution of a viscously heated accretion disk, using the approximation of an optically thick disk [33], using the formula:

$$T(R) = \left\{ \frac{3GM\dot{M}}{8\pi R^3\sigma} \left[1 - \left(\frac{R_*}{R} \right)^{1/2} \right] \right\}^{1/4} \quad (3)$$

We calculated the temperature for each radius between R_{in} and R_{out} , and integrated the Planck law over each area element of the disk to estimate the emitted spectrum.

The modelled emission due to this effect is plotted with green dash-dotted lines in Fig. 5.

- X-ray irradiation of the accretion disk:

In order to model the X-ray irradiation of the accretion disk for each incident L_X along the outburst, for the grid of values of R_{out} described above, we used the relation for $T(R)$ given by Vrtilék et al. [38]:

$$T(R) \approx 23200K \left(\frac{f_2 f_3 \sqrt{f_1}}{0.5} \right)^{2/7} \left(\frac{\dot{M}}{10^{18} g/s} \right)^{2/7} \left(\frac{R_\odot}{R} \right)^{3/7} \quad (4)$$

where f_1 is a factor that depends on the details of the vertical structure of the disk and has been fixed to 1, f_2 is the absorbed fraction of the impinging radiation and has been fixed to 0.5, and f_3 takes into account the possible anisotropy of the radiation and has been fixed to 1.

This contribution is represented with a brown dashed line in Fig. 5.

- X-ray heating of the surface of the companion star:

The irradiation of the surface of the the Be star by the X-ray photons emitted close to the NS can contribute significantly to the optical and UV emission [7, 36]. We have calculated the extra emission in each band by estimating the difference between the emission from an unirradiated O9.5 V star and that from an irradiated star, considering a radius of the donor star of $R_* = 8 R_\odot$, and an initial effective temperature of $T_{\text{eff}} = 32000$ K.

We considered that the X-rays emitted by the NS are absorbed by the atmosphere of the optical companion and then thermally re-radiated at lower energies. We have followed a similar modelling to the one describe in Ducci et al. [9] to estimate the contribution of the heated surface of the Be star on A0538–66. In this model, the X-rays emitted by the central source are absorbed by the atmosphere of the companion star and heat its surface. For each surface element of the star, the local effective temperature increases as:

$$T_e^4 = T_{0,e}^4 + (1 - \eta) \frac{L_X \cos \phi}{4\pi \sigma R^2} \quad (5)$$

with $T_{0,e}^4$ the effective temperature of an unirradiated surface element, η is the albedo (fraction of reflected X-rays) that we have fixed to 0.5, L_X is the X-ray luminosity of the source, ϕ is the angle between the direction to the X-ray source and the normal of the surface element, σ is the Stefan-Boltzmann constant, and R is the distance from the surface element to the X-ray source. We calculated this distance for each phase using the latest orbital parameters.

We have calculated the contribution of this effect for each X-ray luminosity along the outburst. To illustrate this effect, the modelled heating of the surface of the optical companion of Swift J0243.6+6124 at the peak of the outburst (MJD 58064) is shown in Fig. 6. As can be seen, the center of the facing star reaches an extra heating of $\Delta T > 12000$ K.

In our modelling, we assumed that the Be disk was coplanar to the orbit during the outburst, which is the simplest configuration to explain the occurrence of an X-ray outburst in a BeXB system [27]. Under this assumption that the Be disk is co-planar to the orbit, the X-rays would not impinge on the Be disk, since the angles that the X-rays form with the normal vector of the Be disk surface would be close to 90 degrees and then they would not heat the Be disk surface. This is the reason why we neglected this mechanism.

4.2.2 Optical/UV SEDs fits

The optical/UV SEDs built with the available observations along the outburst, together with the best SED fit for each day are plotted in Fig. 7. For those days for which we had optical measurements

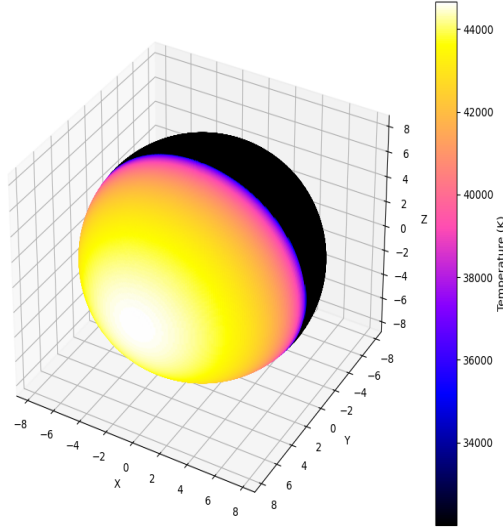


Figure 6: Illustration of the effect of X-ray heating of the surface of the companion star. The calculations for the peak of the outburst (58064 MJD) are shown.

in the V band, we calculated the value of the outer radius of the accretion disk, R_{out} , yielding the best fit of the SED using the minimization of chi-square method (see Fig. 8). The black solid lines represent the sum of the three modelled components. The different mechanisms are plotted with different colours and line styles: the pink dotted lines represent the modelled contribution by the extra emission from heating the surface of the companion star, and the brown dashed lines correspond to the emission modelled from an irradiated accretion disk with the value of R_{out} providing the best fit. The emission from the viscously heated accretion disk is too faint to appear represented in the plot. Since it does not contribute significantly to the optical and UV fluxes and can be ruled out from the discussion.

As can be seen in Fig. 7, the heating of the surface of the companion star (blue dotted line) contributes significantly to the optical and UV observed fluxes along the whole outburst. The SED fits get improved with the addition of an irradiated disk from MJD 58047 to 58120. Before MJD 58047, the heating of the companion star is enough to explain the observed optical/UV emission. However, the irradiation of the accretion disk contributes significantly to the UV emission close during and after the peak of the outburst (from MJD 58062 aprox.).

To reproduce the observed fluxes, we performed two different fits. First, we left the outer radius of the accretion disk (R_{out}) as a free parameter of the fit (see Fig. 8). From the results of the fits, an increasing R_{out} along the outburst is obtained, reaching a value of $R_{out} \sim 0.18a$ at 58097 MJD. After that, a larger value of R_{out} , reaching the upper limit given by the Roche Lobe $R_{out} \sim R_L = 0.20a$, is required to fit the observed optical fluxes from 58100 to 58120 MJD (see Fig. 8). This could be understood as an increase of the size of R_{out} and could be interpreted as

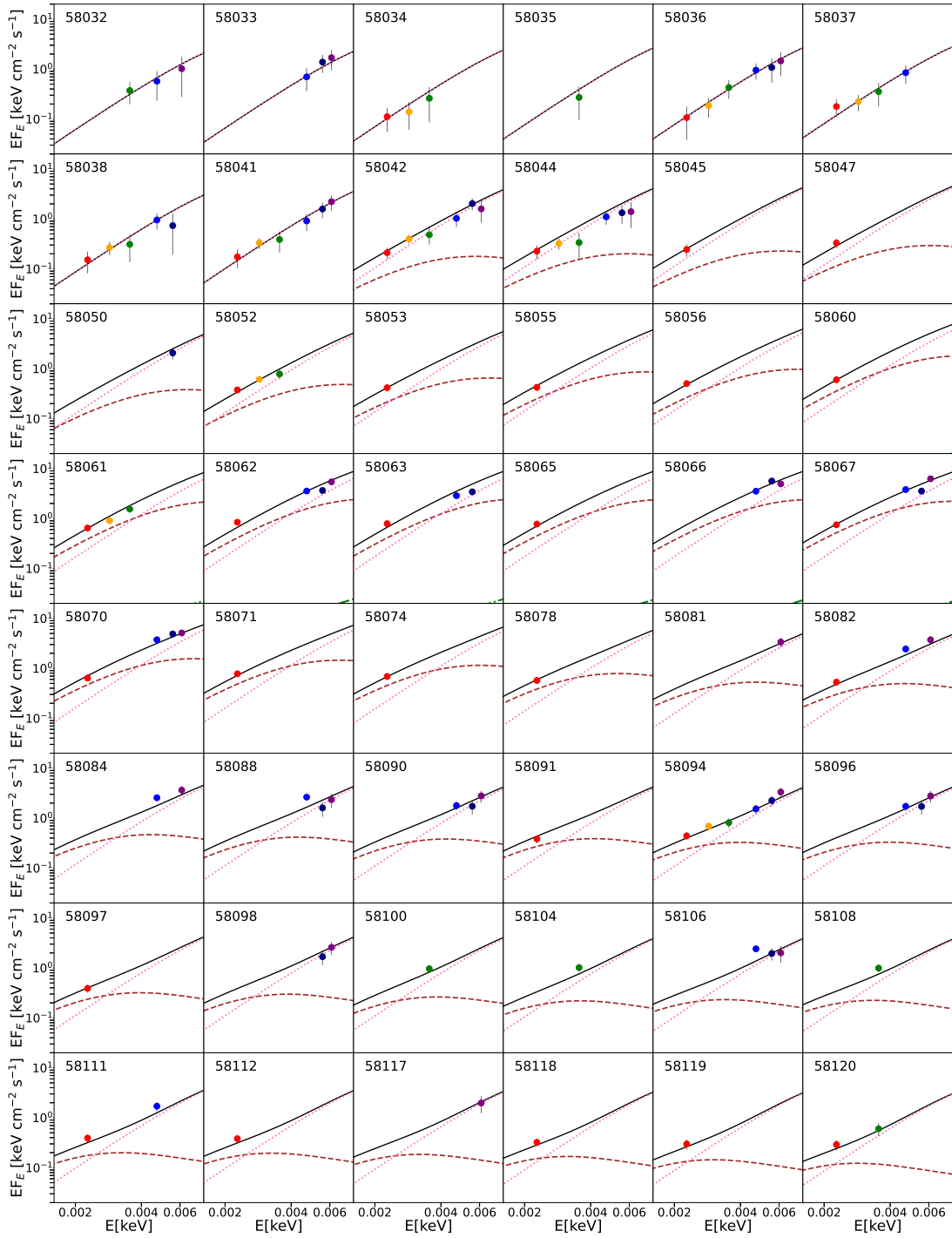


Figure 7: Optical/UV SEDs evolution along the outburst. The reddening corrected observed fluxes are plotted with different colours: *V*-Johnson in red, UVOT-*b* in yellow, UVOT-*u* in green, UVOT-*uw1* in blue, UVOT-*um2* in navy blue, and UVOT-*uw2* in purple. Error bars are plotted in gray. Best fitted model predictions are plotted for comparison (black solid lines). The pink dotted lines represent the modelled contribution by the extra emission from heating the surface of the companion star. The brown dashed lines correspond to the contribution from an irradiated accretion disk with the value of R_{out} providing the best fit.

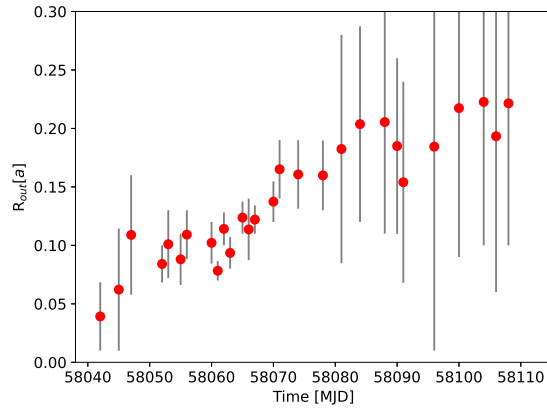


Figure 8: Outer radius of the accretion disk which provided the best fit for each SED.

a progressive increase of the size of the accretion disk or a dissipation towards the outer parts of the disk. We want to stress that for this first attempt, we fixed all the geometrical factors and the fraction of reprocessed emission along the whole outburst, and we only considered R_{out} as a free parameter in our modelling. This increase of the emission contributing to the redder wavelengths along the outburst is in agreement with the differences observed between the rise and decay in the flux-flux correlations for the redder wavelengths (Sect. 3.4).

Such an increase on the redder fluxes could also be reproduced by modifying the factors in the irradiation disk model which depend on the vertical scale of the disk and the effects of possible anisotropy of the radiation, or the fraction of reprocessed emission due to changes in the ionization or the spectra shape (see Eq. 4). Such effects seem to have occurred during this outburst. Doroshenko et al. [8] proposed that during this giant outburst, the system underwent transitions between three states: sub-critical gas pressure dominated disk (GPD), super-critical GPD (dashed blue line in Fig. 3), and super-critical radiation pressure dominated disk (RPD). The times proposed for the transitions between these states are marked as dashed and solid pink lines respectively in Fig. 3. These changes in the geometry of the accretion disk should have an effect on the fraction of reprocessed X-ray emission at longer wavelengths. Moreover, the change from pencil to fan beam regime proposed by Liu et al. [23] also should have a direct impact on the fraction of X-ray flux impinging on the accretion disk due to geometrical effects. It could also happen that the accretion disk gets flared in the outer parts, and this would result in a stronger heating of the disk and a larger contribution to the redder fluxes. Moreover, the X-ray radiation was harder during the decay than during the rise of the outburst (for similar X-ray fluxes), and the albedo is smaller for harder X-rays. A smaller albedo would lead to higher optical/UV emission.

5. Conclusions

We have studied the optical/UV emission of the 2017–2018 giant outburst of the ULXP Swift J0243.6+6124. From the correlation observed between the optical and X-ray fluxes, X-ray reprocessing is proposed to be the origin of the optical/UV emission. We have built a physical

model including three mechanisms: heating of the surface of the donor star, X-ray irradiation of the accretion disk, and thermal emission from a viscously heated accretion disk. We conclude that the first two mechanisms are able to reproduce the observed SEDs and can explain the origin of the optical/UV emission. The complete details of this work, all the figures presented, and a deeper discussion on the obtained results and other possible interpretations can be found in [1].

References

- [1] Alfonso-Garzón, J., van den Eijnden, J., Kuin, N. P. M., et al. 2023, arXiv e-prints, arXiv:2312.08080
- [2] Arnaud, K. A. 1996, in *Astronomical Society of the Pacific Conference Series*, Vol. 101, *Astronomical Data Analysis Software and Systems V*, ed. G. H. Jacoby & J. Barnes, 17
- [3] Bahramian, A., Kennea, J. A., & Shaw, A. W. 2017, *The Astronomer's Telegram*, 10866, 1
- [4] Barthelmy, S. D., Barbier, L. M., Cummings, J. R., et al. 2005, *Space Sci. Rev.*, 120, 143
- [5] Burrows, D. N., Hill, J. E., Nousek, J. A., et al. 2005, *Space Sci. Rev.*, 120, 165
- [6] Bykov, S. D., Gilfanov, M. R., Tsygankov, S. S., & Filippova, E. V. 2022, *MNRAS*, 516, 1601
- [7] Charles, P. A. & Coe, M. J. 2006, in *Compact stellar X-ray sources*, Vol. 39, 215–265
- [8] Doroshenko, V., Tsygankov, S., Long, J., et al. 2020, *A&A*, 634, A89
- [9] Ducci, L., Mereghetti, S., Hryniewicz, K., Santangelo, A., & Romano, P. 2019, *A&A*, 624, A9
- [10] Eggleton, P. P. 1983, *ApJ*, 268, 368
- [11] Evans, P. A., Beardmore, A. P., Page, K. L., et al. 2009, *MNRAS*, 397, 1177
- [12] Fitzpatrick, E. L. 1999, *PASP*, 111, 63
- [13] Fürst, F., Kretschmar, P., Kajava, J. J. E., et al. 2017, *A&A*, 606, A89
- [14] Gehrels, N., Chincarini, G., Giommi, P., et al. 2004, *ApJ*, 611, 1005
- [15] Gierliński, M., Done, C., & Page, K. 2009, *MNRAS*, 392, 1106
- [16] Güver, T. & Özel, F. 2009, *MNRAS*, 400, 2050
- [17] Hayasaki, K. & Okazaki, A. T. 2004, *MNRAS*, 350, 971
- [18] Hayasaki, K. & Okazaki, A. T. 2006, *MNRAS*, 372, 1140
- [19] Jenke, P. & Wilson-Hodge, C. A. 2017, *The Astronomer's Telegram*, 10812, 1
- [20] Kennea, J. A., Lien, A. Y., Krimm, H. A., Cenko, S. B., & Siegel, M. H. 2017, *The Astronomer's Telegram*, 10809, 1

- [21] King, A. R. & Ritter, H. 1998, MNRAS, 293, L42
- [22] Krimm, H. A., Holland, S. T., Corbet, R. H. D., et al. 2013, ApJS, 209, 14
- [23] Liu, J., Jenke, P. A., Ji, L., et al. 2022, MNRAS, 512, 5686
- [24] Liu, W., Yan, J., Reig, P., et al. 2022, A&A, 666, A110
- [25] Malacaria, C., Jenke, P., Roberts, O. J., et al. 2020, ApJ, 896, 90
- [26] Moritani, Y., Nogami, D., Okazaki, A. T., et al. 2013, PASJ, 65, 83
- [27] Okazaki, A. T., Bate, M. R., Ogilvie, G. I., & Pringle, J. E. 2002, MNRAS, 337, 967
- [28] Reig, P. 2011, Astrophysics and Space Science, 332, 1
- [29] Reig, P., Fabregat, J., & Alfonso-Garzón, J. 2020, A&A, 640, A35
- [30] Rivinius, T., Carciofi, A. C., & Martayan, C. 2013, Astronomy and Astrophysics Review, 21, 69
- [31] Roming, P. W. A., Kennedy, T. E., Mason, K. O., et al. 2005, Space Sci. Rev., 120, 95
- [32] Rykoff, E. S., Miller, J. M., Steeghs, D., & Torres, M. A. P. 2007, ApJ, 666, 1129
- [33] Shakura, N. I. & Sunyaev, R. A. 1973, A&A, 500, 33
- [34] van den Eijnden, J., Degenaar, N., Russell, T. D., et al. 2018, Nature, 562, 233
- [35] van Paradijs, J. & McClintock, J. E. 1994, A&A, 290, 133
- [36] van Paradijs, J. & McClintock, J. E. 1995, in X-ray Binaries, 58–125
- [37] Verner, D. A., Ferland, G. J., Korista, K. T., & Yakovlev, D. G. 1996, ApJ, 465, 487
- [38] Vrtilik, S. D., Raymond, J. C., Garcia, M. R., et al. 1990, A&A, 235, 162
- [39] Wilms, J., Allen, A., & McCray, R. 2000, ApJ, 542, 914
- [40] Wilson-Hodge, C. A., Malacaria, C., Jenke, P. A., et al. 2018, ApJ, 863, 9
- [41] Yan, J., Li, H., & Liu, Q. 2012, ApJ, 744, 37
- [42] Zhang, Y., Ge, M., Song, L., et al. 2019, ApJ, 879, 61